GN-model-based SNR Estimation in 15.2-THz Bandwidth Inline-amplified Transmission with 80-km Fibre Spans

Kosuke Kimura(1), Takayuki Kobayashi(1), Shimpei Shimizu(1), Masanori Nakamura(1), Takushi Kazama(1,2), Masashi Abe(2), Takeshi Umeki(1,2), Akira Kawai(1), Fukutaro Hamaoka(1), Yutaka Miyamoto(1)

(1) NTT Network Innovation Laboratories, NTT Corporation, 1-1 Hikarinooka, Yokosuka, Kanagawa, Japan, kousuke.kimura@ntt.com
(2) NTT Device Technology Laboratories, NTT Corporation, 3-1 Morinosato, Wakamiya, Atsugi, Kanagawa, Japan

Abstract *We validated <1-dB-mean-absolute GN-model-based SNR estimation errors against experimentally measured SNRs in 15.2-THz ultra-wideband transmission over 160- and 400-km G.652.D fibre consisting of 80-km spans with PPLN-based optical parametric inline amplifiers. We found gain equalization for increasing the total throughput using SNR estimation. ©2023 The Author(s)*

Introduction

To cope with ever-increasing traffic demand, ultra-wideband (UWB) wavelength division multiplexing (WDM) technologies beyond C- and L-bands have been investigated [1]-[7]. One of the challenges with UWB WDM systems is inter-channel stimulated Raman scattering (ISRS) [8], which transfers signal power from shorter wavelengths to longer wavelengths. ISRS complicates the optimization of the launch power of WDM signals to fibre spans, which is determined by a combination of fibre Kerr-effects and amplified spontaneous emission (ASE) from inline amplifiers. So far, experimental [9] and numerical [10] optimization techniques have been reported for UWB systems. The numerical technique involves signal to noise ratio (SNR) estimations using a closed-form Gaussian noise (GN) model accounting for ISRS, which enables fast estimations of nonlinear interference (NLI). The high computational efficiency of the closed-form GN models is attractive for enabling the design of UWB WDM systems that require complex power optimization. However, only a few experimental studies such as [10], [11] have been conducted to validate the accuracy of SNR estimations using closed-form GN models for transmission beyond the C+L bands. [10], [11] reported experimental validations of S+C+L-band transmission up to 200 km (2 spans). These experiments used doped fibre amplifiers for the S- and C-band and semiconductor optical amplifiers for the L-band as lumped inline repeaters.

In this study, first, we validate SNR estimation with a closed-form GN model [12] by comparing estimated SNRs with measured SNRs from our previously reported transmission experiment over 160- and 400-km G.652.D fibre consisting of 80-km spans [13]. In this experiment, periodically poled $LiNbO_3$ (PPLN)-based optical parametric amplifiers (OPAs) with a 14.1-THz amplification bandwidth (the bandwidth including the guard band was 15.2 THz) were used as a lumped inline repeater. The WDM signal was composed of 103-channel 132-Gbaud probabilistic-constellation-shaped (PCS)-QAM signals. We demonstrate that the mean absolute errors between the estimated and experimentally measured SNRs are less than 1 dB after 160- and 400-km transmission. Then, we optimize the gain equalization on the basis of SNR estimation to increase the total throughput based on generalized mutual information (GMI). We reveal that the total throughput can increase by 2.5 and 1.6 Tb/s for 160- and 400-km transmission, respectively, by optimizing gain equalization.

Numerical calculation

Figure 1 shows our system model corresponding to the experimental setup in [13].

At the transmitter, each channel power of the WDM signal into the re-circulating transmission line was calculated. The WDM signal contained 103 137.5-GHz-spaced channels, consisting of 48 shorter-band channels (1490.75–1541.34 nm) and 55 longer-band channels (1549.36–1612.34 nm). The entire bandwidth including the guard band between both bands was 15.2 THz, which was beyond the Raman shift frequency. The modulation format was 132-Gbaud PCS-QAM. The input power of each channel to the re-circulating transmission line was pre-equalized by optical gain equalizer (GEQ) 1 so that the optical spectrum before an 80-km G.652.D fibre agreed with the experimentally measured optical spectrum before the fibre span shown in Fig. 1 (d). The signal powers after GEQ1 were 0.32 dBm in the shorter band and −3.0 dBm in the longer band. The total signal power was 2.0 dBm.

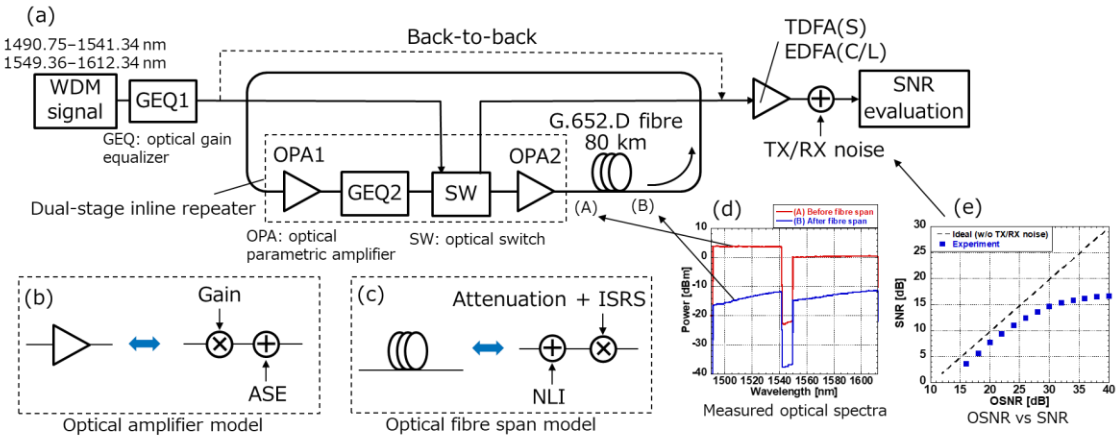

Fig. 1: (a) System model to estimate SNRs, (b) optical amplifier model, (c) optical fibre span model, (d) measured optical spectra before and after 80-km G.652.D fibre, and (e) OSNR (noise bandwidth = 0.1 nm) vs SNR characteristic.

The re-circulating transmission line consisted of an 80-km fibre span and an inline repeater including OPA1 and 2, GEQ2, and an optical switch (SW). OPA1 and 2 were modelled as shown in Fig. 1 (b): multiplying the gain and then adding ASE to the signal. The model used the experimentally measured gain and noise figure (NF) shown in Figs. 2 (a) and (b). GEQ2, between OPA1 and 2, equalized the signal power so that the optical spectrum after OPA2 matched at each lap. The attenuation of the SW was set to 2.0 dB. The fibre span of 80 km was modelled as shown in Fig. 1 (c): adding NLI and then multiplying the fibre attenuation and ISRS gain or loss to the signal [14]. NLI was estimated by using a closed-form GN model accounting for ISRS [12]. This model estimates NLI including self-channel interference (SCI) and cross-channel interference (XCI). The approximated coherence term of the SCI in the GN model was ignored in this calculation because its contribution to the total NLI seems relatively small for G.652.D fibre and a 103-channel WDM signal over 15.2 THz [15], [16]. ISRS was estimated by solving coupled Raman equations [17]. The NLI and ISRS estimation procedures used the following fibre parameters: a nonlinear coefficient of 1.2 $W^{-1}km^{-1}$ (treated as wavelength-independent), dispersion at 1550 nm for 17 ps/nm/km, and dispersion slope at 1550 nm for 0.067 $ps/nm^2/km$ [18]. Figures 3 (a) and (b) show the attenuation and Raman gain coefficient spectra of the G.652.D fibre. The attenuation spectrum was experimentally measured. The Raman gain coefficient spectrum was calculated while regarding the shortest wavelength channel as a pump channel. Similarly, Raman gain coefficients for other wavelength pump channels were calculated. The wavelength dependence of the coefficients was considered as in [19]. The fibre input powers for the shorter and longer bands were set to 20.6 dBm (~3.8 dBm/channel) and

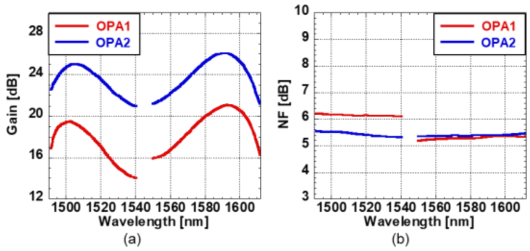

Fig. 2: OPA characteristics. (a) Gain, (b) NF.

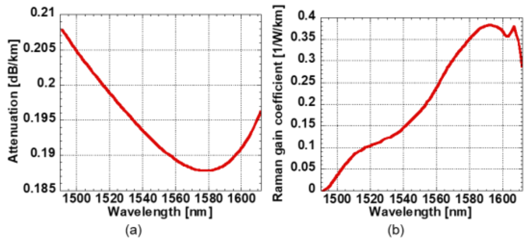

Fig. 3: G.652.D fibre characteristics. (a) Attenuation, (b) Raman gain coefficient for lowest wavelength channel.

18.1 dBm (~0.7 dBm/channel).

After the re-circulating transmission line, the WDM signal was amplified by different preamplifiers for each S-, C-, and L-band. The NFs were set to 7.0 dB for the S-band, 4.2 dB for the C-band, and 5.2 dB for the L-band. The NFs were averaged measured values of the S-band TDFA, C-band EDFA, and L-band EDFA used in the experiment. Subsequently, the SNR including TX/RX noise was calculated by converting the generalized optical signal to noise ratio (GOSNR), which included the accumulated ASE and NLI at a 0.1-nm noise bandwidth, to the SNR according to Fig.1 (e). Figure 1 (e) shows an OSNR vs SNR characteristic experimentally measured at a 1550.98-nm channel in the back-to-back configuration. The SNRs were estimated from the variance of the recovered symbols. The OSNR vs SNR characteristic was used for all the channels.

Results and discussion

Figure 4 shows attenuation spectra with ISRS for the 80-km G.652.D fibre. For comparison, attenuation without ISRS is also shown by the dotted line. The red and blue lines correspond to the attenuation spectra experimentally measured and estimated by solving the coupled Raman equations, respectively. The measured and estimated attenuation spectra agreed well, demonstrating that ISRS was accurately estimated. The ISRS loss on the shorter-band side and ISRS gain on the longer-band side were about 3.5 dB.

Figures 5 (a), (b), and (c) show SNRs of all WDM channels in the back-to-back configuration, after the 160- and 400-km transmission. The square and circle plots correspond to the experimental and numerical results. Even with an attenuation tilt of about 7 dB across the signal bandwidth shown in Fig. 4, the wavelength dependence of the SNRs was similar to the inverse of the gain characteristics of the OPAs shown in Fig. 2, suggesting that GEQ2 or the ASE from OPA2 largely affected the SNRs. The mean absolute errors of the estimated SNRs were 0.40, 0.56, and 0.92 dB in the back-to-back configuration, after the 160- and 400-km transmission, respectively. The increase in the estimation errors for longer transmission distances seemed to result from the imperfection of GEQ2. Although the maximum estimation error after the 400-km transmission (5 re-circulations) in the shorter band was 2.33 dB, this error could arise from a difference of only 0.46 dB (= 2.33/5) in the gain equalization. These indicate that the estimated SNRs almost agreed with the experimentally measured SNRs.

Finally, we examined the conditions superior for increasing the total throughput on the basis of calculation. Because the ASE from OPA2 dominated the SNRs, we changed GEQ1 and 2 and optimized the input spectrum to OPA2. The average power of the OPA2 input WDM signal was fixed (0 dBm) to avoid significant deviation from the experimentally validated condition. The OPA2 input spectrum was changed by multiplying GEQ for OPA2 by a coefficient, X. X = 1 corresponds to the unchanged GEQ. Figure 6 (a) shows OPA2 input spectra for $X = -1, -0.5, 0, 0.5$, and 1. Figure 6 (b) shows corresponding GMI throughputs of the WDM channels after the 160-km transmission. The GMI throughputs after the 400-km transmission were also calculated but are not shown due to limited space. Figures 6 (c) and (d) show the total throughputs after the 160- and 400-km transmission. The total throughputs peaked at $X = 0$. The total throughputs at $X = 0$ outnumbered those at $X = 1$ (before the optimization) by 2.5 and 1.6 Tb/s for the 160- and 400-km transmission. These results indicate that flattening the OPA2 input spectrum can increase the total throughput. This means that the throughput gain from improving low SNR channels outweighs the throughput loss from worsening high SNR channels.

Conclusion

We demonstrated that the mean absolute errors of the estimated SNRs were less than 1 dB in 15.2-THz inline-amplified 160- and 400-km transmission with 80-km spans. Using GN-model-based SNR estimation, we revealed that the total throughput could increase by 2.5 and 1.6 Tb/s for 160- and 400-km transmission by flattening the OPA2 input spectrum under the constraint of a fixed OPA2 input power.

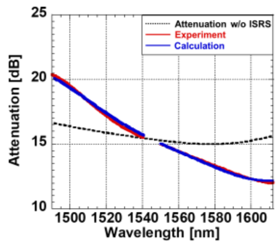

Fig. 4: Attenuation spectra of 80-km G.652.D fibre.

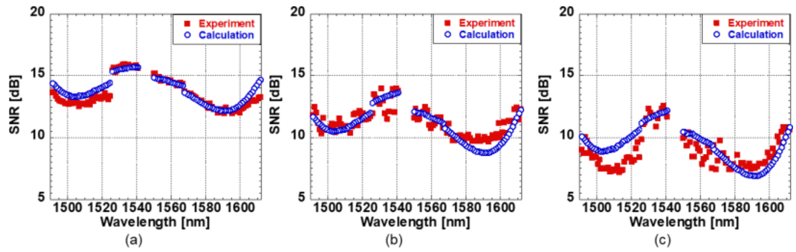

Fig. 5: SNRs of WDM channels (a) in back-to-back configuration, (b) after 160- and (c) 400-km transmission.

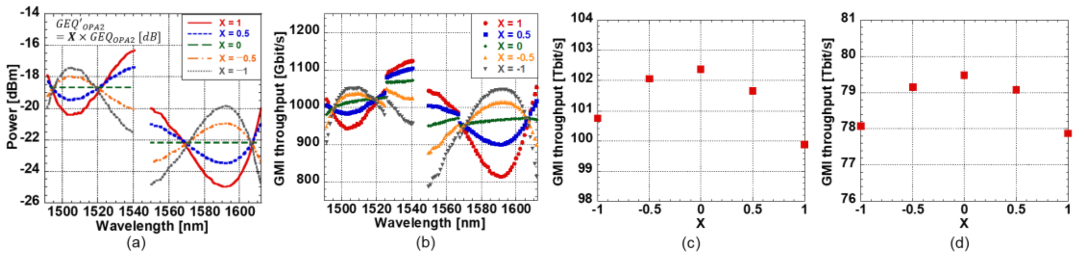

Fig. 6: Optimizing GEQ to increase total throughput. (a) OPA2 input spectra, (b) estimated throughputs of WDM channels after 160-km transmission, and (c) and (d) estimated total throughputs after 160- and 400-km transmission.

References

[1] S. Okamoto, K. Minoguchi, K. Horikoshi, A. Matsushita, M. Nakamura, E. Yamazaki, and Y. Kisaka, “A study on the effect of ultra-wide band WDM on optical transmission systems,” in Journal of Lightwave Technology, vol. 38, no. 5, pp. 1061-1070, March 1, 2020, doi: 10.1109/JLT.2019.2962178.

[2] T. Kobayashi, S. Shimizu, M. Nakamura, T. Umeki, T. Kazama, R. Kasahara, F. Hamaoka, M. Nagatani, H. Yamazaki, H. Nosaka, and Y. Miyamoto, “Wide-band inline-amplified WDM transmission using PPLN-based optical parametric amplifier,” in Journal of Lightwave Technology, vol. 39, no. 3, pp. 787-794, Feb. 1, 2021, doi: 10.1109/JLT.2020.3039192.

[3] B. J. Puttnam, R. S. Luís, G. Rademacher, Y. Awaji, and H. Furukawa, “Investigation of long-haul S-, C- + L-band transmission,” 2022 Optical Fiber Communications Conference and Exhibition (OFC), San Diego, CA, USA, pp. 1-3, 2022.

[4] R. Emmerich, M. Sena, R. Elschner, C. Schmidt-Langhorst, I. Sackey, C. Schubert, and R. Freund, “Enabling S-C-L-band systems with standard C-band modulator and coherent receiver using nonlinear predistortion,” in Journal of Lightwave Technology, vol. 40, no. 5, pp. 1360-1368, March 1, 2022, doi: 10.1109/JLT.2021.3123430.

[5] F. Hamaoka, K. Saito, A. Masuda, H. Taniguchi, T. Sasai, M. Nakamura, T. Kobayashi, and Y. Kisaka, “112.8-Tb/s real-time transmission over 101 km in 16.95-THz triple-band (S, C, and L Bands) WDM configuration,” 2022 27th OptoElectronics and Communications Conference (OECC) and 2022 International Conference on Photonics in Switching and Computing (PSC), Toyama, Japan, pp. 1-3, 2022, doi: 10.23919/OECC/PSC53152.2022.9849881.

[6] T. Kato, H. Muranaka, Y. Tanaka, Y. Akiyama, T. Hoshida, S. Shimizu, T. Kobayashi, T. Kazama, T. Umeki, K. Watanabe, and Y. Miyamoto, “WDM transmission in S-band using PPLN-based wavelength converters and 400-Gb/s C-band real-time transceivers,” 2022 27th OptoElectronics and Communications Conference (OECC) and 2022 International Conference on Photonics in Switching and Computing (PSC), Toyama, Japan, pp. 01-04, 2022, doi: 10.23919/OECC/PSC53152.2022.9849997.

[7] X. Zhao, S. Escobar-Landero, D. Le Gac, A. Lorences-Riesgo, T. Viret-Denaix, Q. Guo, L. Gan, S. Li, S. Cao, X. Xiao, N. El Dahdah, A. Gallet, S. Yu, H. Hafermann, L. Godard, R. Brenot, Y. Frignac, and G. Charlet, “200.5 Tb/s transmission with S+C+L amplification covering 150 nm bandwidth over 2×100 km PSCF spans,” 2022 European Conference on Optical Communication (ECOC), Basel, Switzerland, pp. 1-4, 2022.

[8] K. Minoguchi S. Okamoto, F. Hamaoka, A. Matsushita, M. Nakamura, E. Yamazaki, and Y. Kisaka, “Experiments on stimulated Raman scattering in S- and L-bands 16-QAM signals for ultra-wideband coherent WDM systems,” 2018 Optical Fiber Communications Conference and Exposition (OFC), San Diego, CA, USA, pp. 1-3, 2018.

[9] F. Hamaoka et al., “Ultra-wideband WDM transmission in S-, C-, and L-Bands using signal power optimization scheme,” in Journal of Lightwave Technology, vol. 37, no. 8, pp. 1764-1771, April 15, 2019, doi: 10.1109/JLT.2019.2894827.

[10] S. E. Landero, X. Zhao, A. L. Riesgo, D. L. Gac, Y. Frignac, and G. Charlet, “Modeling and optimization of experimental S+C+L WDM coherent transmission system,” 2023 Optical Fiber Communications Conference and Exhibition (OFC), San Diego, CA, USA, 2023.

[11] S. E. Landero, X. Zhao, D. L. Gac, A. L. Riesgo, T. V. Denaix, Q. Guo, L. Gan, S. Li, S. Cao, X. Xiao, I. Demirtzioglou, N. E. Dahadh, A. Gallet, S. Yu, H. Hafermann, L. Godard, R. Brenot, Y. Frignac, and G. Charlet, “Demonstration and characterization of high-throughput 200.5 Tbit/s S+C+L transmission over 2x100 PSCF spans,” in Journal of Lightwave Technology, doi: 10.1109/JLT.2023.3266926.

[12] M. Ranjbar Zefreh and P. Poggiolini, “A real-time closed-form model for nonlinearity modeling in ultra-wide-band optical fiber links accounting for inter-channel stimulated Raman scattering and copropagating Raman amplification,” arXiv:2006.03088, June 2020.

[13] T. Kobayashi, S. Shimizu, M. Nakamura, T. Kazama, M. Abe, T. Umeki, A. Kawai, F. Hamaoka, M. Nagatani, H. Yamazaki, and Y. Miyamoto, “103-ch. 132-Gbaud PS-QAM signal inline-amplified transmission with 14.1-THz bandwidth lumped PPLN-based OPAs over 400-km G.652.D SMF,” 2023 Optical Fiber Communications Conference and Exhibition (OFC), San Diego, CA, USA, 2023.

[14] V. Curri, “GNPy model of the physical layer for open and disaggregated optical networking [Invited],” in Journal of Optical Communications and Networking, vol. 14, no. 6, pp. C92-C104, June 2022, doi: 10.1364/JOCN.452868.

[15] P. Poggiolini, “The GN model of non-linear propagation in uncompensated coherent optical systems,” in Journal of Lightwave Technology, vol. 30, no. 24, pp. 3857-3879, Dec. 15, 2012, doi: 10.1109/JLT.2012.2217729.

[16] M. Ranjbar Zefreh, F. Forghieri, S. Piciaccia, and P. Poggiolini, “Accurate closed-form real-time EGN model formula leveraging machine-learning over 8500 thoroughly randomized full C-band systems,” in Journal of Lightwave Technology, vol. 38, no. 18, pp. 4987-4999, Sept. 15, 2020, doi:10.1109/JLT.2020.2997395.

[17] S. Tariq and J. C. Palais, “A computer model of non-dispersion-limited stimulated Raman scattering in optical fiber multiple-channel communications,” in Journal of Lightwave Technology, vol. 11, no. 12, pp. 1914-1924, Dec. 1993, doi: 10.1109/50.257951.

[18] D. Semrau, R. I. Killey, and P. Bayvel, “A closed-form approximation of the Gaussian noise model in the presence of inter-channel stimulated Raman scattering,” in Journal of Lightwave Technology, vol. 37, no. 9, pp. 1924-1936, May 1, 2019, doi: 10.1109/JLT.2019.2895237.

[19] K. Kimura, S. Shimizu, T. Kobayashi, T. Kazama, K. Enbutsu, T. Umeki, and Y. Miyamoto, “Accurate estimation of inter-channel stimulated Raman scattering in C+L+U ultra-wideband WDM systems beyond Raman shift frequency,” 2023 28th OptoElectronics and Communications Conference (OECC) and 2023 International Conference on Photonics in Switching and Computing (PSC), Shanghai, China, 2023.